Understanding anthropogenic methane and carbon dioxide point source emissions

Riley M. Duren[1], Andrew K. Thorpe[1], Robert O. Green[1], Christian Frankenberg[2], David R. Thompson[1], Andrew D. Aubrey[1], Charles E. Miller[1], Kevin R. Gurney[3], Luis Guanter[4], Heinrich Bovensman[5], Konstantin Gerilowski[5], Ilse Aben[6], Andre Butz[7], Colm Sweeney[8], Eric A. Kort[9]

[1]Jet Propulsion Laboratory, California Institute of Technology
[2]California Institute of Technology
[3]Arizona State University
[4]Helmholtz-Zentrum Potsdam Deutsches GeoForschungsZentrum
[5]University of Bremen
[6]SRON Netherlands Institute for Space Research
[7]Karlsruhe Institute of Technology
[8]NOAA/CU Boulder
[9]University of Michigan

I. Science and Application Targets and their importance in addressing Decadal Survey themes and previous community roadmaps, and advancing understanding

Understanding the processes controlling changes in atmospheric methane (CH_4) and carbon dioxide (CO_2) is at the core of Earth System Science and two Decadal Survey themes: Climate Change (radiative forcings) and Air Quality (atmospheric chemistry). These gases are the two dominant anthropogenic climate-forcing agents. Additionally CH_4 is relevant to air-quality science and applications: CH_4 is a precursor for tropospheric ozone and is strongly linked with co-emitted reactive trace gases that are the focus of air quality mitigation policies. The atmospheric growth rates are strongly influenced by anthropogenic emissions of CH_4 and dominated by fossil fuel CO_2 emissions from a population of spatially condensed point sources distributed over large areas and spanning diverse socio-economic sectors. However, especially for CH_4, bottom-up estimates are often in strong disagreement with top-down estimates and our lack of process based knowledge is exemplified by the ongoing scientific discussion on both the hiatus in the atmospheric growth rate in the early 21st century as well as the unexpected rise starting in 2007. Emissions and process attribution remain highly uncertain but are needed to resolve key elements of the key elements of uncertainty in carbon cycle science, generate accurate greenhouse gas inventories and inform emission mitigation decisions. A key factor is that regional top-down emissions estimates cannot discriminate source categories and thereby attribute fluxes to specific processes or sources.

One way of solving this knowledge gap is by isolating anthropogenic point sources from regional totals. The impact of anthropogenic CH_4 point sources – principally from coal, oil and gas supply chains, manure and waste management – on the atmospheric CH_4 growth rate is significant. However the relative contribution compared to natural (wetland) and other anthropogenic area sources (e.g., enteric fermentation) has not been conclusively resolved (Turner et al., 2015; Shaefer et al., 2016; others). Uncertainty in CH_4 emissions remains persistently large at all scales and process attribution remains challenging as well (Kirschke et al., 2013). Hypotheses regarding the space-time distribution of anthropogenic CH_4 point source fluxes have only been partially tested due to observational limitations. For example, recent field studies of CH_4 emissions from oil and gas supply chains in the US provide compelling evidence of super-emitter (fugitives with long-tail distribution) behavior (Zavala-Araiza et al., 2015; Brandt et al., 2014; Lyon et al., 2015; Frankenberg et al., under review). However, while those studies offer spatially complete assessments and some indication of stochastic leak behavior they lack the vantage point with persistent, high frequency sampling and broad area

coverage necessary to constrain the distribution of episodic emission processes. There is a need to complete similar assessments in I) other coal, oil and gas regions around the world (only a subset of which are accessible by airborne campaigns) and II) important but under-sampled CH_4 emission sectors such as manure and waste management. The same limitations pose barriers to providing relevant and timely information to decision-makers seeking to mitigate emissions (e.g., leak detection and repair).

Historically, global fossil fuel CO_2 (FFCO2) emissions were considered one of the better known terms in the carbon budget – constraining less well known terms such as the terrestrial land sink (Cox et al., 2013). However, this was largely driven by a limited quantitative understanding of $FFCO_2$ uncertainties and the fact that the global total uncertainty was dominated by the lower uncertainty of the high-income countries. Given that the global FFCO2 emissions contain a larger proportional share of emissions from historically less-developed economies, uncertainty is growing significantly and will continue to do so over the coming years. The FFCO2 uncertainty is already comparable in magnitude to uncertainty in the natural land sink (GCP, 2015). Over 50% of the world's CO_2 emissions come from tens of thousands of power plants and other industrial facilities including many where information regarding their emissions or even their locations is not readily available - translating to large (or unquantified) flux uncertainties at local scales (NRC, 2010).

We suggest an observational strategy focused on CH_4 and CO_2 point source emissions with three goals aligned with US Carbon Cycle Science Program priorities (CCSP, 2011):

1. Enable explanation of past and current variations in atmospheric CO_2 and CH_4 (CCSP goal 1)
2. Understand and quantify socioeconomic drivers of carbon emissions, and develop transparent methods to monitor and verify emissions (CCSP goal 2)
3. Address decision maker needs for carbon-cycle information with actionable data –including direct guidance for near-term and longer-term mitigation action (CCSP goal 6)

To achieve those goals we suggest a **Quantified Earth Science and Applications Objective**:
Reduce uncertainty in the individual emission fluxes of anthropogenic CH_4 and fossil fuel CO_2 point sources (with diameters ≤ 100 m) to ≤ 20% (CO_2) and 50% (CH_4) (2σ) for 90% of the global source populations of those point sources[1]; geo-locate those sources to within 30 meters to support process attribution; persistently monitor the source population for super-emitter behavior including large episodic emissions; and produce flux estimates within 1 week of detecting CH_4 threshold-crossing events to enable timely mitigation action.

Justification: The global point source population for fossil fuel CO_2 emissions consists of tens of thousands of power plants and other industrial facilities and for CH_4, tens of millions of potential point sources distributed across oil and gas supply chains, large agricultural facilities and waste-management facilities associated with major cities. Reducing uncertainties in point source fluxes from the current large or unquantified levels to 20% (CO_2) to 50% (CH_4) in all key sectors and regions will significantly reduce global CO_2 and CH_4 uncertainties. Providing fine-scale source geolocation is necessary both for general emissions accounting and for unambiguous process attribution in crowded source environments. Persistent monitoring for potential episodic emissions (i.e., leaks) and low latency notification will enable rapid repair action particularly for CH_4 sources.

II. Utility of the measured geophysical variables to achieving the science/application target

We propose a tiered observational strategy focused on CH_4 and CO_2 point source fluxes at fine-space time scales sufficient to detect, quantify and attribute them, and to provide timely information to facility operators and other decision makers. This approach would both complement and bridge gaps

[1] Definition of source populations, spatial completeness, and flux uncertainty targets are degrees of freedom that can be adjusted and balanced as needed to address different science/application priorities, cost and schedule. The numbers presented in this whitepaper are notional and intended to illustrate key concepts and trade-space.

in planned observational systems focusing on area sources (Fig. 1). The tiered strategy would deploy satellites and coordinated aircraft surveys with very high spatial resolution (5 to 30 m) observations of CH_4 and CO_2 column mole fractions with persistent, dense sampling of key anthropogenic infrastructure. The strategy involves three tiers to provide flexibility in meeting the objective – both in terms of timeliness and preserving the opportunity to employ multiple vantage points, platforms, and partnerships between instrument- and data-providers:

Tier-1: Global mapping of all land surfaces leveraging existing instrument hardware (potential launch by 2019) with a focus on CO_2 from power plants and other major industrial facilities and CH_4 from the largest anthropogenic point sources. The global coverage is particularly important to determining the locations of the largest fossil fuel CO_2 emitting facilities.

Tier-2: Annual aircraft campaigns over known CH_4 point source infrastructure using existing and new instrument technology (potential first flight before 2020) in key regions globally with sufficient sensitivity to detect >80% of emissions.

Tier-3: Global high-frequency sampling of the majority of known CH_4 and CO_2 point source infrastructure using new instrument technology (potentially launched by 2022) with sufficient sensitivity to rapidly detect super-emitters and inform timely mitigation action.

Table 1 traces our Quantified Earth Science and Applications Objective to requirements on data products, instruments and sampling approaches for satellite and aircraft platforms.

Table 2 summarizes the utility of these measurements to meeting our science and applications targets and provides context by comparing with other reference missions.

III. The key requirements on the quality (i.e. the performance and coverage specifications) of the measurement(s) needed for achieving the science and application target.

Passive remote spectroscopy is a powerful tool to characterize trace greenhouse gas emissions (Kort et al., 2014; Schneising et al 2015; Turner et al 2015). While current and planned carbon monitoring satellites promise significant advances in reducing uncertainty for regional and area sources of CO_2 and CH_4 (Schimel et al., 2015) they were not designed to detect or quantify anthropogenic point source fluxes or their controlling processes. These limitations are primarily due to coarse spatial resolution (typically instrument native resolutions of several kilometers and flux inversion resolutions of 10 to >100 km; CEOS, 2014). Spatial resolution impacts both detection sensitivity (since point source plumes disperse rapidly, dilution scales with pixel size) and geolocation (point sources often appear in crowded scenes). For example, existing and planned satellites such as GOSAT and TROPOMI/Sentinel-5P have nadir footprints of 85 km^2 and 49 km^2, respectively. Compared to an instrument with 10 meter pixels, GOSAT and TROPOMI both experience a factor of >100,000 degradation in sensitivity to spatially condensed point source plumes due simply to pixel size. Hence even less precise imaging spectrometers will produce dramatically improved sensitivity to point source plumes compared to traditional greenhouse gas sounders. Additionally, existing and planned observational systems often provide sample frequencies measured in weeks to months given their focus on regional to continental scale fluxes. Even satellites with "global daily revisit" capability will in practice achieve sample frequencies measured in days to weeks for pixel sizes much larger than 1 km due to cloud interference (Bloom et al., 2016). Compared to traditional atmospheric sounders, high resolution imaging spectrometers will have greater sampling density and frequency resulting in a higher cloud free yield. *In fact, the two approaches are synergistic; observing systems focused on area sources address other distinct and important aspects of regional and global carbon cycle science (Schimel et al 2015).* A focus on fine scale point sources uniquely extends and complements these observational capabilities (Fig. 1), greatly enhancing both systems' science yield and societal applications.

In the past few years, rapid progress has been made in detecting and quantifying CH_4 plumes with high spatial resolution using prior airborne instruments. The airborne imaging spectrometers AVIRIS-C and AVIRIS-NG measure reflected solar radiation between 380 and 2,500 nm at 10 and 5 nm spectral resolution (Green et al., 1998; Hamlin et al., 2011). While not designed for this application, they have successfully mapped CH_4 and CO_2 emissions (Roberts et al., 2010; Thorpe et al., 2014; Thompson et al., 2015; Spinetti et al., 2004; Dennison et al., 2013). Examples of quantitative gas retrievals using optical absorption spectroscopy (Frankenberg et al., 2005, under review) with AVIRIS-NG are shown for CH_4 emissions from a gas processing plant with good agreement between measured and modelled radiances (Fig. 2) and CO_2 emissions from a coal-fired power plant (Fig. 3). A recent study used AVIRIS-C and the Hyperion orbital instrument (6.6 and 30 m spatial resolution, respectively) to observe CH_4 plumes from the Aliso Canyon leak over multiple days (Fig. 4). To our knowledge this represents the first orbital detection of an individual CH_4 point source (Thompson et al., 2016, under review).

A limitation with existing imaging spectrometers is the moderate spectral resolution, which can cause interferences between surface and atmospheric features. A 1 nm spectral resolution would eliminate this (Krings et al., 2013) and achieve sufficient CH_4 and CO_2 sensitivity while maintaining an imaging capability and the fine spatial resolution required to resolve individual emission sources (Thorpe et al., 2014; Thorpe et al., 2016). This improved sensitivity is illustrated in Fig. 5 where CH_4 and CO_2 Jacobians are plotted for a 10 nm (AVIRIS), 5 nm (AVIRIS-NG), and 1 nm spectral resolution instrument. Plume modeling combined with a simulated atmosphere and retrieval algorithms reveal which gas fluxes are detectable for different design points. A 5 nm spectral and 30 m spatial resolution results in an estimated CH_4 flux detection threshold of 1,000 kg/h, while for a 1 nm spectral and 10 m spatial resolution the threshold falls to 50 kg/hr. An airborne imaging spectrometer that was designed exclusively for quantitative mapping of CH_4 and CO_2 (Thorpe et al., 2016) could further reduce detection thresholds and complement orbital instruments (Fig. 6). For example, an instrument with 1 nm spectral resolution flying at 5 km above ground (5 m spatial resolution) results in a detection threshold around 10 kg/h (and 0.5 kg/h at 1 km altitude). The importance of spatial and spectral resolution favors a three tiered system with different instrument/measurement requirements to resolve different aspects of the emission profile (Table 1). Tier 1 would utilize a Landsat–like sun-synchronous orbit with global terrestrial coverage, an image swath of 185 km, and a 16 day revisit interval[2]. Its 30 m spatial and 5 nm spectral sampling would be capable of detecting larger fluxes, targeting detection thresholds of 1,000 kg CH_4/hr and 200,000 kg CO_2/hr. These thresholds correspond to the largest known CH_4 emitters (contributing 30% of total emissions from sampled population) and the largest CO_2 emitting power plants and other industrial facilities (contributing 80% of total fossil fuel CO_2 emissions) – see Table 2. Tier 1's global coverage would not rely on prior knowledge of facility locations. Tier 2 would use airborne measurements (1 nm spectral, 5 m spatial resolution, 5 km swath) to conduct bi-annual surveys of sources populations in key regions to detect small CH_4 and CO_2 sources. Tier 3 would use a constellation of small sats carrying imaging spectrometers with 10 m spatial resolution, 1 nm spectral sampling and a revisit interval of 3 days to monitor the much larger population of potential CH4 sources including super-emitters with fluxes as small as 50 kg/hr (Table 2) and rapidly notify facility operators and decision makers of episodic threshold crossing events. Tier 2 and 3 measurements would permit detection of a significant portion of emissions from key oil and gas basins as documented in previous studies (Lyon et al., 2015; Zavala-Araiza et al., 2015;). For both tier 1 and tier 3, spacecraft pointing could be used to target specific regions of interest. All three tiers would benefit from simplified plume modeling and available wind information to estimate fluxes rather than depending on atmospheric transport models required for flux inversions using sparser observations over larger areas (Frankenberg et al., under review).

[2] Revisit intervals described here refer to the cloud-free sample frequency defined by the spacecraft orbit assumed for these notional cases.

IV. Likelihood of affordably achieving the required measurements in the decadal timeframe given the maturity of instruments, algorithms, and the potential for partnerships

Investments in response to global terrestrial/coastal coverage missions outlined in the 2007 NRC Decadal Survey (NRC 2007), the NRC *Landsat and Beyond* report (NRC, 2013), and other initiatives will ensure that the required measurements can be achieved affordably in the decadal timeframe. They would build on a legacy of imaging spectrometers designed for airborne and orbital applications. For airborne instruments, spectral resolution has improved from 10 nm for AIS (Vane et al., 1984) and AVIRIS (Green et al., 1998), to 5 nm for AVIRIS-NG (Hamlin et al., 2011), and to 3 nm for PRISM (Mouroulis et al., 2014). Orbital measurements using imaging spectrometers have been successfully demonstrated with NIMS (Carlson et al., 1992), VIMS (Brown et al., 2004), Deep Impact (Hampton et al., 2005), CRISM (Murchie et al., 2007), EO-1 Hyperion (Ungar et al, 2003; Middleton et al., 2013), M3 (Green et al., 2011), and MISE, the imaging spectrometer now being developed for NASA's planned Europa mission.

NASA-guided engineering studies determined that a Landsat-class VSWIR (380 to 2,510 nm @ ≤10 nm sampling) imaging spectrometer instrument with a 185 km swath, 30 m spatial sampling and 16 day revisit with high signal-to-noise ratio and the required spectroscopic uniformity could be implemented affordably for a three year mission with mass (98 kg), power (112 W), and volume compatible with a Pegasus class launch (Fig. 7). The instrument design and a technology demonstration (high TRL) is complete, featuring an optically fast spectrometer with high SNR that accommodates the full spectral and spatial ranges (Mouroulis et al., 2016) and a scalable prototype F/1.8 full VSWIR spectrometer (Van Gorp et al., 2014) is currently being qualified (Fig. 8).

Lossless compression algorithms for spectral measurements (Klimesh et al., 2006; Aranki et al., 2009ab; Keymeulen et al., 2014) will permit the required data transfer rate and this algorithm is currently a CCSDS standard (CCSDS, 2015). Using compression and the current Ka band downlink offered by KSAT and others, all terrestrial/coastal measurements can be downlinked. Algorithms for calibration (Green et al., 1998) and atmospheric correction (Gao et al., 1993, 2009; Thompson et al., 2014, 2016) have been applied to large, diverse data sets as part of the HyspIRI preparatory campaign (Lee et al., 2015) as well as AVIRIS-NG India and Greenland campaigns. CH_4 and CO_2 retrieval algorithms are mature (Thorpe et al., 2014, 2016; Thompson et al., 2015) and have been applied in near real time to large data sets including surveys of the San Juan Basin, CA (Thompson et al., 2015) and the Four Corners region (Frankenberg et al., under review). This offers the promise of onboard data processing to reduce demands on satellite data storage and downlink systems.

There are a number of existing or planned instruments with fine spatial resolution (Hyperion, EnMAP, Landsat Swath Spectrometer), however, these were not designed for CH_4 and CO_2 mapping. Dedicated orbital imaging spectrometers with improved spectral and spatial resolution will be critical for understanding CH_4 and CO_2 growth rates, balancing the carbon budget, and improving greenhouse gas inventories. High spatial resolution quantitative mapping of emissions will complement existing and planned instruments that provided global and regional measurements at coarser spatial resolutions, like TROPOMI (CH_4 at 49 km^2 resolution) and OCO-2 (CO_2 at 2.9 km^2 resolution). Airborne instruments will also be required with far finer spatial resolution that will result in improved sensitivities (Thorpe et al., 2016).

Finally, the tiered observing strategy described here would provide flexibility for staged sequential deployment of observing capability – beginning with existing instrument hardware for tier 1. New instrument technology would be applied as soon as it completed development and testing (tiers 2 and 3). The multi-platform/instrument approach for tiers 2 and 3 allows for partnering between US agencies, international partners, and potentially the private sector. This could in turn contribute to a coordinated constellation of small satellites (and/or aircraft) with incrementally deployed observing capability while managing cost and risk.

V. Tables and Figures

Table 1. Traceabilty Matrix showing flow down of science and application targets to Quantitative Earth Science Objective and requirements on data products, measurement/observational strategy and instrument requirements. These requirements are notional and intended to illustrate the trade space that could be explored for optimal performance or implementation flexibility.

Decadal Survey themes	Science & Application Targets	Quantitative Earth Science Objective	Tier	Data Product Requirements	Measurement Requirements	Instrument Requirements
1. Climate Change (forcings) 2. Air Quality (atmospheric chemistry)	1. Enable explanation of past and current variations in atmospheric CO2 and CH4 (CCSP goal 1) 2. Understand and quantify socioeconomic drivers of carbon emission, transparent methods to monitor and verify emissions (CCSP goal 2) 3. Address decision maker needs for carbon-cycle information with actionable data - including direct guidance for near-term and longer-term mitigation action (CCSP goal 5)	Reduce uncertainty in the individual emission fluxes of anthropogenic CH4 and fossil fuel CO2 point sources (with diameters <= 100m) to <= 20% (CO2) and 50% (CH4) (2σ) for 90% of the global source populations of those point sources; geo-locate those sources to within 30 meters to support process attribution; persistently monitor the source population for super-emitter behavior including large episodic emissions; and produce flux estimates within 1 week of detecting CH4 threshold-crossing events to enable timely mitigation action.	1	D1. Database of emission fluxes from large stationary fossil-fuel CO2 point sources comprising >80% of global emissions from those sectors	M1. Persistent monitoring of global land surface with <= 3 monthly revisit interval. M2. Detect sources with 200,000 kgCO2/hr threshold (2.5 m/s wind) M3. Flux estimation precision <= 20%	Type: Imaging Spectrometer Mode: global mapping Platform: single satellite Spatial resolution: 30m Swath width: 180 km FWHM: 5 nm Wavelength: 1.9 - 2.5 micron
				D2. Database of emission fluxes from the largest CH4 super-emitter point sources comprising 80% of potential global point source population with rapid notification.	M4. Persistent monitoring of global land surface with <= 3 monthly revisit interval. M5. Detect sources with 1000 kgCH4/hr threshold (2.5 m/s wind) M6. Flux estimation precision <= 50% M7. Flux estimation latency <= 30 days.	
			2	D3. Bi-annual CH4 Assessment Report for key regions comprising 90% of potential regional point source population.	M8. Airborne survey for a *Methane Point Source Population* in specified region(s)[2] M9. Detect sources with 10 kgCH4/hr threshold (2.5 m/s wind) M10. Flux estimation latency <= 3 days (following overflight).	Type: Imaging Spectrometer Mode: regional mapping Platform: aircraft (N/region) Spatial resolution: 5m Swath width: 5 km FWHM: 1 nm Wavelength: 1.9 - 2.5 micron
			3	D4. Database of emission fluxes from large stationary fossil-fuel CO2 point sources comprising 99% of global emissions from those sectors	M11. Persistent monitoring of FFCO2 *Point Source Population*[1] with <= 2 week revisit interval. M12. Detect sources with 20,000 kgCO2/hr threshold (2.5 m/s wind) M13. Flux estimation precision <= 20%	Type: Imaging Spectrometer Mode: global mapping[3] & targeted sampling[4] Platform: Smallsat constellation Spatial resolution: 10m Daily sampling: 250,000 km2 (target mode) FWHM: 1 nm Wavelength: 1.9 - 2.5 micron
				D5. Database of emission fluxes from CH4 super-emitter point sources comprising 80% of potential global point source population with rapid notification.	M14. Persistent monitoring of CH4 *Point Source Population2* with <= 2 week revisit interval. M15. Detect sources with 500 kgCH4/hr detection threshold (2.5 m/s wind) M16. Flux estimation precision <= 50% M17. Flux estimation latency <= 30 days.	

1. Fossil Fuel CO2 Point Source Population: largest power plants and industrial facilities globally (tens of thousands)
2. Methane Point Source Population: ~100,000 known large point sources & total population of ~10,000,000 facilities over ~10 key regions whose total emissions may be dominated by a relatively small (<=10%) but unknown subset
3. Global mapping with relaxed detection threshold (vs requirements M12 and M15)
4. Targeted sampling with detection thresholds as specified in M12 and M15.

Table 2. Preliminary estimates of point source detection performance for the proposed 3 tiers of the CH_4 observing system with other existing (OCO-2, Crisp et al., 2004), planned (TROPOMI, Veefkind et al., 2012; EnMAP, Kaufmann et al., 2016) and proposed (CarbonSat, Buchwitz et al., 2013) systems for reference. The fraction of total emissions from each source population is based on spatial coverage, detection threshold, and representative emission distribution curves from the indicated literature and data sources (see footnotes). Detection thresholds are based on a variety of analyses and in some cases (e.g., TROPOMI and OCO-2) simple scaling based on relative native resolutions; a more complete analysis is required to confirm these. Sample interval is approximate but indicates likely measurement yield (expressed as practical time between samples) based on orbit/campaign revisit interval and cloud cover (e.g., for a 2 week revisit we assume practical sample interval of 30 days). The Tier 3 performance assumes a constellation of 16 smallsats.

Observing System	Source population	Fraction of population sampled	Fraction of total emissions from sampled population (for the given detection threshold)	Detection threshold (kg/hr)	Native resolution (m)*	Sample interval** (days)
Tier1	CO2: tens of thousands of facilities (global)[1a]	99%	>80%	200,000	30	30
	CH4: 10,000,000 facilities[1b] (global)	99%	30%	1,000	30	30
Tier2	Ch4: 1,000,000 facilities[2] (limited to key regions)	>90%	90%	10	5	730
Tier3	CO2: tens of thousands of facilities[1a] (global)	>50%	>90%	20,000	10	15
	CH4: 10,000,000 facilities (global)[2]	>50%	50-90%[3]	50	10	15
OCO-2	CO2: tens of thousands of facilities[1a] (global)	<1%	<1%	2,000,000	2,000	30
TROPOMI	CH4: 100,000 known large facilities (global)[1b]	~20%	<10%	20,000	7,000	10
EnMAP	CH4: 100,000 known large facilities (global)[1b]	0.20%	<1%	1,700	30	30
CarbonSat	CO2: tens of thousands of facilities[1a] (global)	~20%	99%	2,000,000	2,000	3
	CH4: 100,000 known large facilities (global)[1b]	~25%	30%	2,300	2,000	3

1a Of 21,000 large power plants in the CARMA database, 30% (~7000 plants) are responsible for 99% of CO2 emissions from that sector; there are also thousands of other industrial facilities that are large CO2 emitters

1b An estimated 10,000,000 facilities globally; only ~100,000 facilities contribute 30% of methane point source emissions (scaled from USEPA GHGRP)

2 Assume super-emitter distibution (scaled from USEIA data and Zavala-Araiza et al, 2015; Lyon et al, 2015; Frankenberg et al, 2016)

3 predict 50-90% completeness with the cited detection threshold (varies by sector)

*native resolution of the instrument (pixel size) not necessarily flux estimate resolution (which is often larger for area source sounders)

**rough estimate of sample interval based on orbit/campaign driven revisit interval and the impact of clouds, northern hemisphere summer

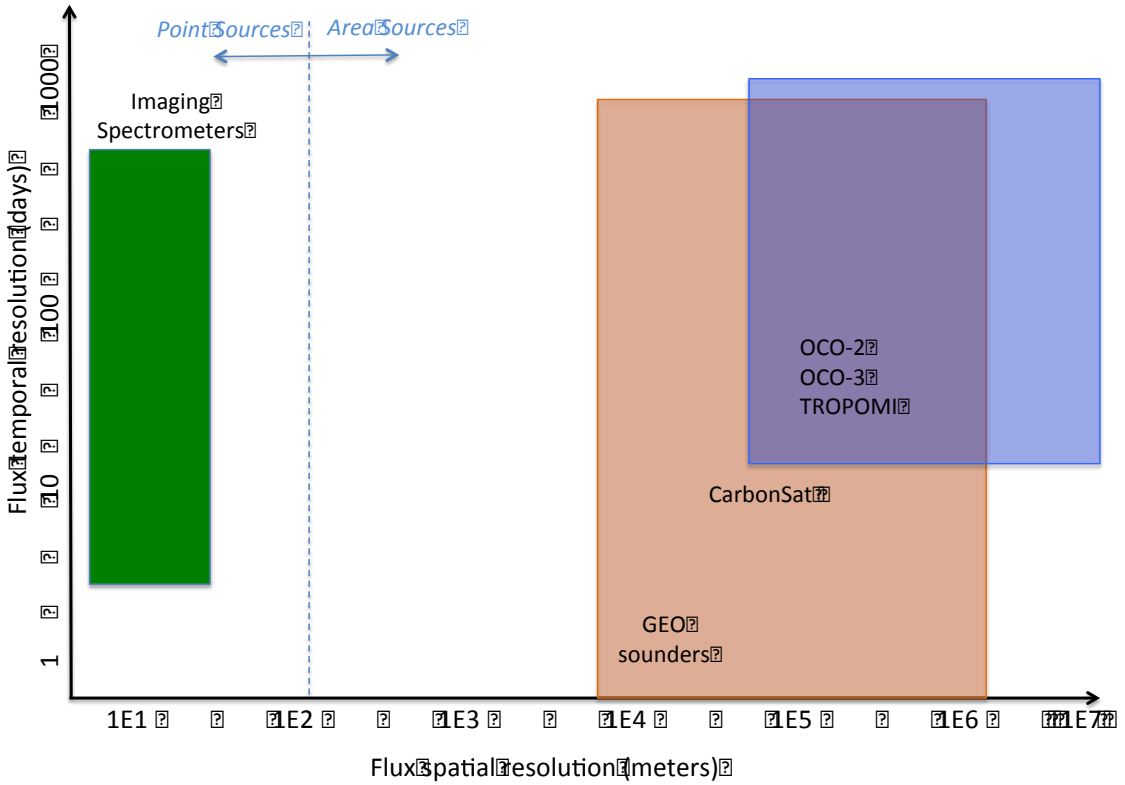

Figure 1. Relative space-time scales for CH_4 and/or CO_2 *flux estimates** generated by observing systems focused on point sources (smaller than about 100 m) compared with those designed to study area sources (>> 100m). The green box represents the range of space-time scales encompassed by the proposed three-tiered point source monitoring system – including satellite and aircraft contributions. The blue box illustrates typical flux space-time scales for representative current and planned satellites/instruments (OCO-2 and OCO-3 for CO_2, TROPOMI for CH_4). The brown box does the same for proposed geostationary CO_2 and CH_4 sounders. Flux estimates from the proposed CarbonSat mission would bridge the gap between the latter two domains. A point source observing system would complement area source measurements and fill gaps at unique space-time scales for carbon cycle science and applications. *[*Unlike most area source observing systems where the space-time resolution of flux estimates is often dominated by the resolution of the atmospheric transport models required for flux inversions, at the scale of individual point source plumes the flux resolution often approaches the native pixel resolution of the instrument. Point source flux estimation can be achieved with simplified estimation methods including Gaussian plume models and publically available wind data rather than the more complex inverse modeling approaches needed at larger spatial scales].]*

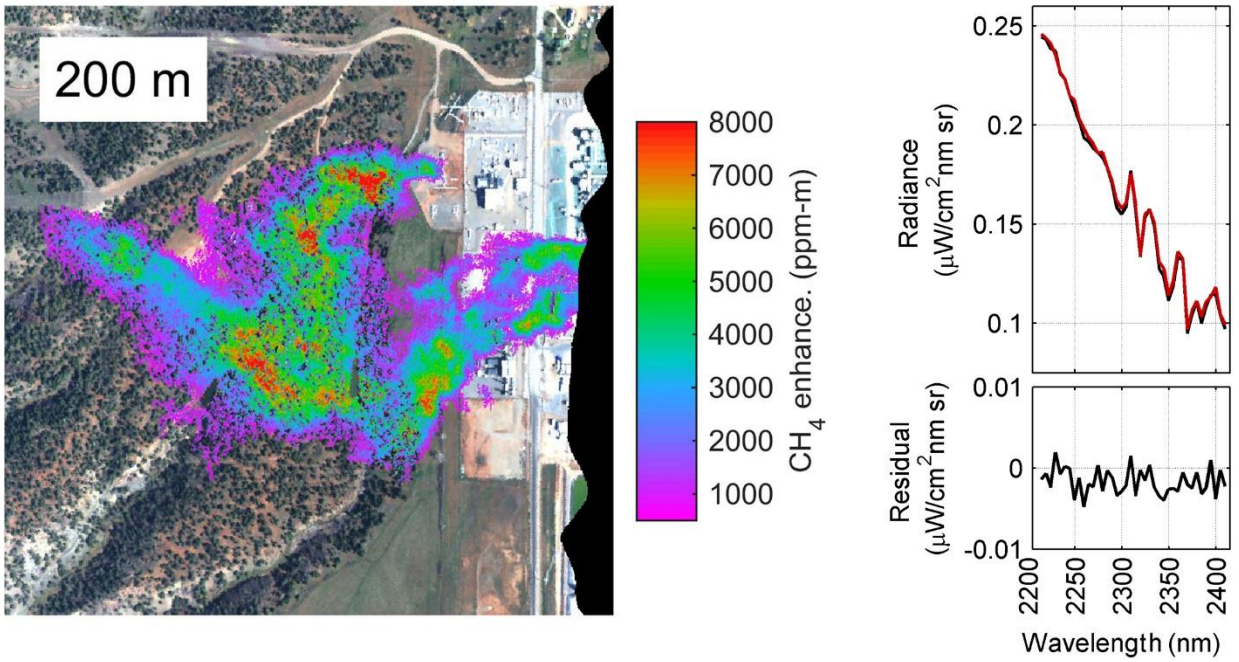

Figure 2. CH_4 plumes observed with AVIRIS-NG flying at 3 km above ground level (3 m pixels). Plume is overlain on true color image showing one emission source for a gas processing plant within the scene and another plume originating from outside the image. Plumes are consistent with local wind conditions, extends 600 m downwind, and has an estimated flux of 6,100 kg/h (Frankenberg et al., under review). IMAP-DOAS CH_4 retrieval shows good agreement between observed radiance (black) and modelled radiance (red).

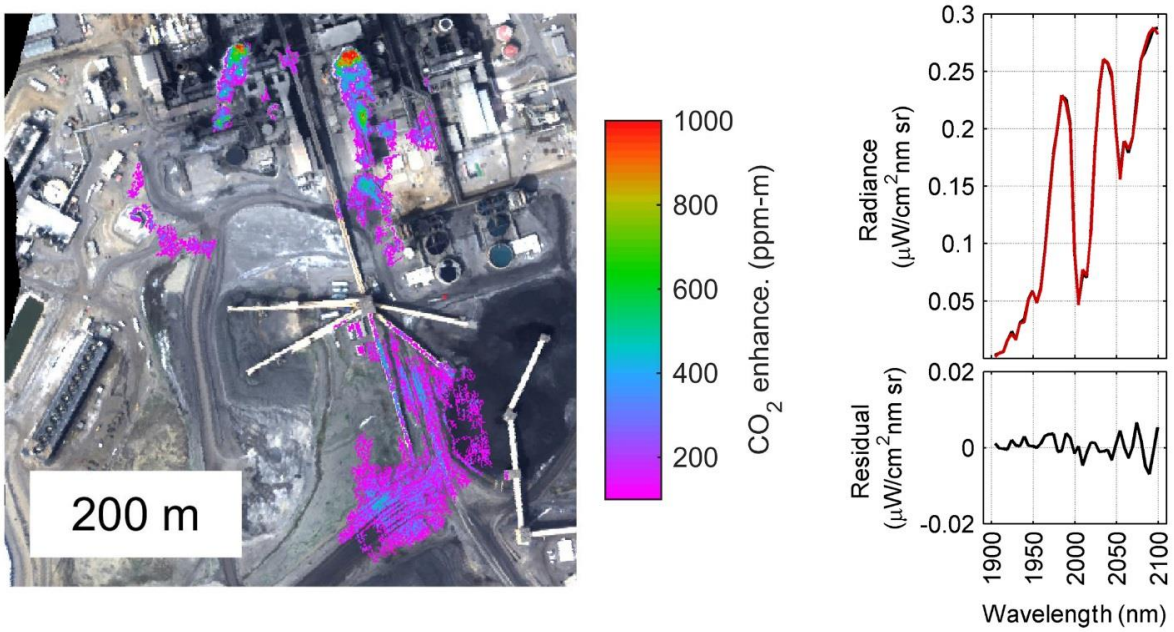

Figure 3. CO_2 plumes observed with AVIRIS-NG flying at 3 km above ground level (3 m pixels). Plume is overlain on true color image showing one emission source for a coal-fired power plant. Plumes are consistent with local wind conditions, extends over 400 m downwind, and has maximum enhancements in excess of 1,000 ppm-m. IMAP-DOAS CH_4 retrieval shows good agreement between observed radiance (black) and modelled radiance (red).

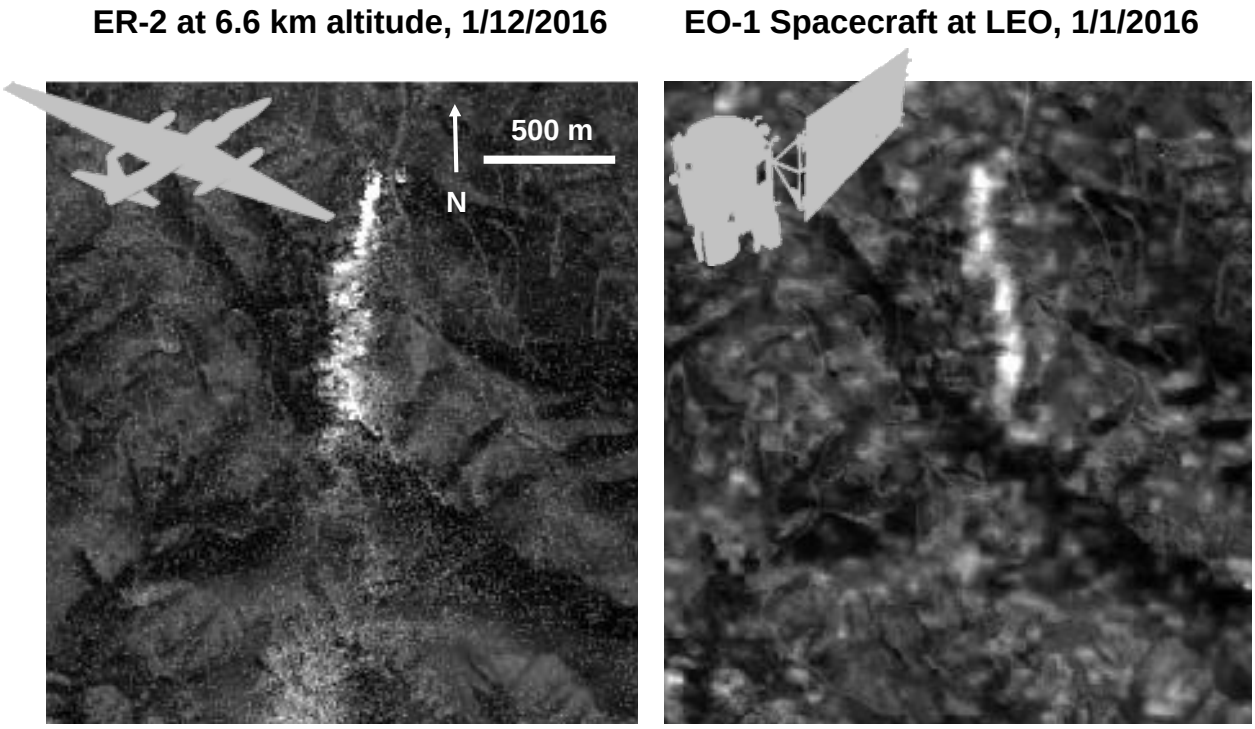

Figure 4. Left: CH_4 plume observed from the Aliso Canyon natural gas leak in January 2016 using AVIRIS-C flying in an ER-2 aircraft at 6.6 km above ground level (6.6 m pixels). Plume is overlayed on the 2,300 nm channel and is consistent with local wind conditions. Right: CH_4 plume observed with the orbital Hyperion instrument onboard the EO-1 spacecraft (30 m resolution) has similar morphology. The EO-1 spacecraft exhausted its fuel in 2011 and the Hyperion spectrometer was disadvantaged by low signal to noise ratio and a solar elevation under 25° (Thompson et al., under review).

Figure 5. CH_4 and CO_2 Jacobians shown for 1, 5, and 10 nm spectral resolution (SR) and full width at half maximum (FWHM). Finer spectral resolution improves gas sensitivity, as shown by the increasing distance between the peaks and troughs of absorption features.

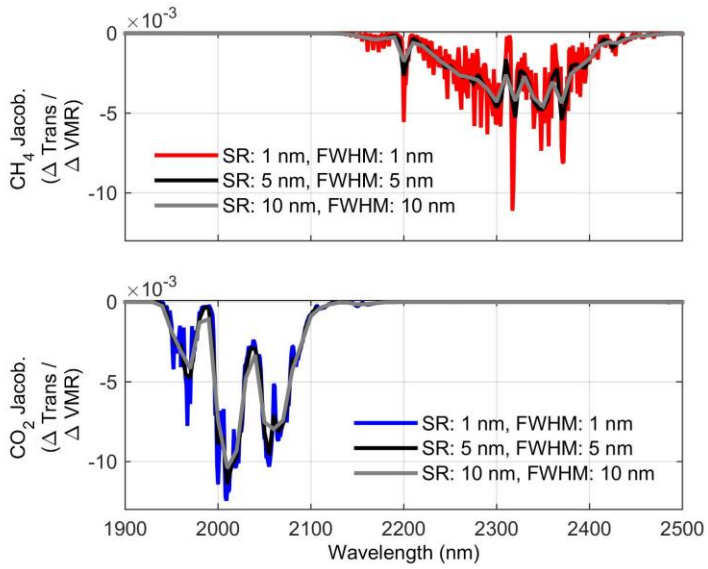

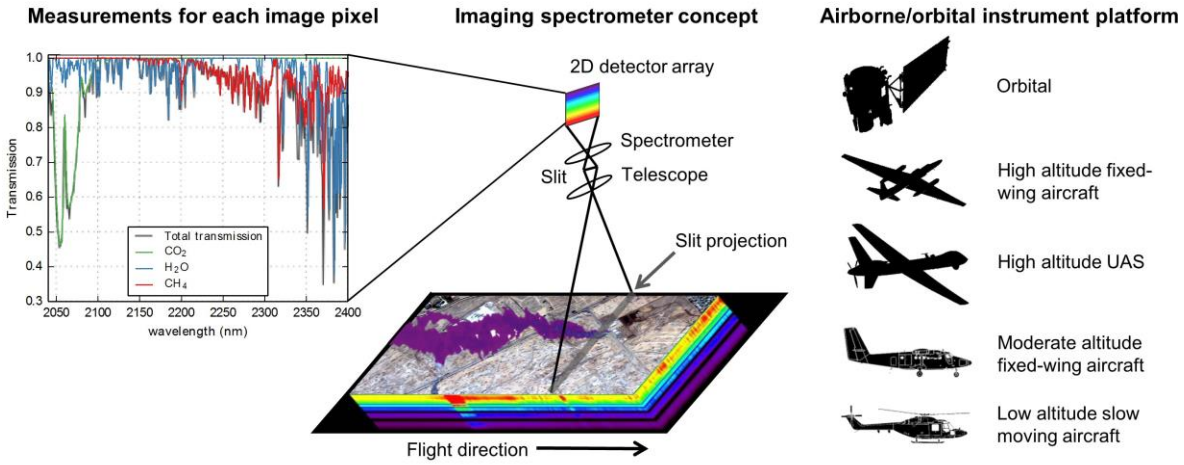

Figure 6. Imaging spectrometer concept showing a pushbroom design with 1 nm spectral sampling that enables high sensitivity measurements for each image pixel. Instrument design would be compatible with a variety of airborne/orbital platforms. Currently, AVIRIS-C and AVIRIS-NG use moderate and high altitude fixed-wing aircraft only.

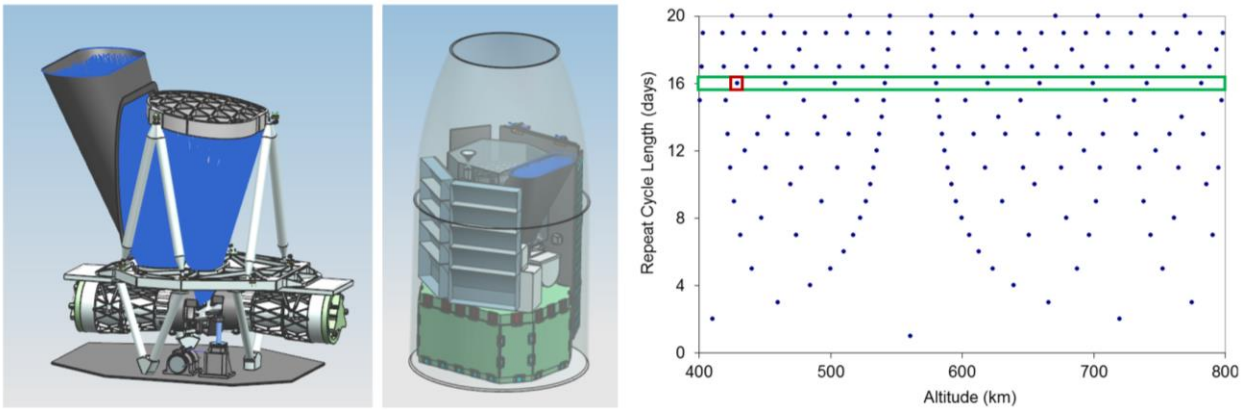

Figure 7. Left: Opto-mechanical configuration with one telescope feeding two field split wide swath F/1.8 VSWIR Dyson spectrometer providing 185 km swath and 30 m sampling. Center: Imaging spectrometer with spacecraft (248 kg, 670 W with margin) configured for launch in a Pegasus shroud for an orbit of 429 km altitude, 97.14 inclination to provide 16 day revisit for three years. Right: Orbital altitude and repeat options showing an altitude of 429 km with a fueled spacecraft supports the three year mission with the affordable Pegasus launch. Higher orbits are viable with a larger launch vehicle.

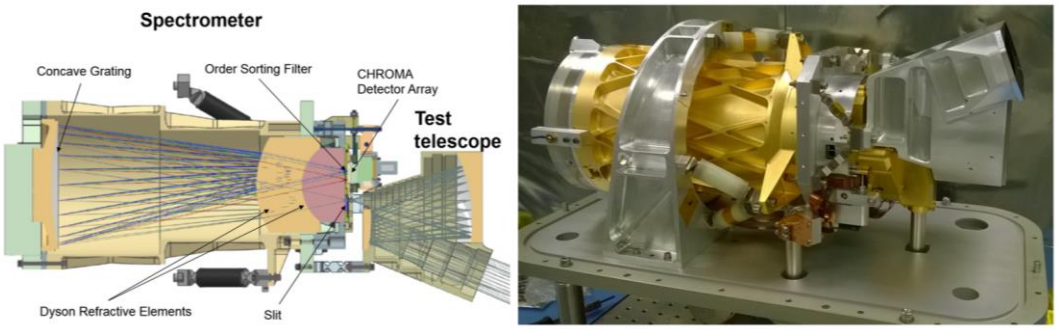

Figure 8. Left: Design of a wide swath F/1.8 VSWIR Dyson covering the spectral range from 380 to 2510 (see Fig. 7). The visible range is not required for this application but is heritage with the as-built instrument. Right: Dyson imaging spectrometer completed for technology demonstration (TRL 5) that uses a full spectral range HgCdTe detector array.

VI. References

Aranki, N., A. Bakshi, D. Keymeulen, and M. Klimesh (2009a). Fast and adaptive lossless onboard hyperspectral data compression system for space applications, 2009 IEEE Aerospace Conf., 7-14 March. doi:10.1109/AERO.2009.4839534.

Aranki, N., D. Keymeulen, A. Bakshi, and M. Klimesh (2009b). Hardware implementation of lossless adaptive and scalable hyperspectral data compression for space, NASA ESA Conf. Adap. Hardware Sys., 29 July – 1 Aug. doi:10.1109/AHS.2009.66.

Bloom, A. A., Lauvaux, T., Yadav, V., Duren, R., Sander, S., Worden, J., and Schimel, D.: What are the greenhouse gas observing system requirements for reducing fundamental biogeochemical process uncertainty? Amazon wetland CH4 emissions as a case study, Atmos. Chem. Phys. Discuss., doi:10.5194/acp-2016-325, in review, 2016.

Brandt, A. R., G. A. Heath, et al. (2014). "Methane Leaks from North American Natural Gas Systems." Science 343(6172): 733-735.

Brown, R. H., Baines, K. H., Bellucci, G., Bibring, J. P., Buratti, B. J., Capaccioni, F., & Drossart, P. (2004). The Cassin Visual and Infrared Mapping Spectrometer (VIMS) Investigation.," Space Science Reviews 115: 111–168, 2004.

Buchwitz, M., Reuter, M., Bovensmann, H., Pillai, D., Heymann, J., Schneising, O., ... & Gerbig, C. (2013). Carbon Monitoring Satellite (CarbonSat): assessment of scattering related atmospheric CO2 and CH4 retrieval errors and first results on implications for inferring city CO2 emissions. Atmospheric Measurement Techniques, 6(12), 3477-3500.

Carlson, R. W., Weissman, P. R., Smythe, W. D., & Mahoney, J. C., "Near-Infrared Mapping Spectrometer experiment on Galileo, "Space Science Reviews (ISSN 0038-6308), vol. 60, no. 1-4, May 1992, p. 457-502.

CARMA (2015). Carbon Monitoring for Action (CARMA) Database, data from www.carma.org.

CCSDS, "LOSSLESS MULTISPECTRAL AND HYPERSPECTRAL IMAGE COMPRESSION INFORMATIONAL REPORT," CCSDS 120.2-G-1, GREEN BOOK, 2015, http://public.ccsds.org/publications/archive/120x2g1.pdf.

CEOS (2014), Committee on Earth Observations, CEOS Strategy for Carbon Observations from Space, figure 4-3.

CCSP (2011). Michalak AM, Jackson RB, Marland G, Sabine CL, Anderson RF, Bronk D, Davis KJ, DeFries RS, Denning AS, Dilling L, Jacobson A. A US carbon cycle science plan. In Nova Science Publishers, Inc. 2013.

Cox, P.M., Pearson, D., Booth, B.B., Friedlingstein, P., Huntingford, C., Jones, C.D., Luke, C.M. (2013). Sensitivity of tropical carbon to climate change constrained by carbon dioxide variability. Nature 494, 341–344.

Crisp, D., Atlas, R. M., Breon, F. M., Brown, L. R., Burrows, J. P., Ciais, P., ... & Miller, C. E. (2004). The orbiting carbon observatory (OCO) mission. Advances in Space Research, 34(4), 700-709.

Dennison, P.E., Thorpe, A.K., Pardyjak, E.R., Roberts, D.A., Qi, Y., Green, R.O., Bradley, E.S., & Funk, C.C. (2013). High spatial resolution mapping of elevated atmospheric carbon dioxide using airborne

imaging spectroscopy: Radiative transfer modeling and power plant plume detection. *Remote Sensing of Environment, 139*, 116-129.

EPA (2016). U.S. Greenhouse Gas Reporting Program (GHGRP), data from EPA's FLIGHT Tool, http://ghgdata.epa.gov/ghgp.

Frankenberg et al. (2016). Unraveling the 4-Corners methane hotspot. Manuscript under review.

Frankenberg, C., Platt, U., & Wagner, T. (2005). Iterative maximum a posteriori (IMAP)-DOAS for retrieval of strongly absorbing trace gases: Model studies for CH4 and CO2 retrieval from near infrared spectra of SCIAMACHY onboard ENVISAT. *Atmospheric Chemistry and Physics, 5*, 9-22.

GCP (2015). Global Carbon Budget 2015. Earth Syst. Sci. Data, 7, 349–396.

Gao, B.-C., K. Heidebrecht, and A. Goetz (1993). Derivation of scaled surface reflectances from AVIRIS data, Remote Sens. of Environ., 44, 165-178. doi:10.1016/0034- 4257(93)90014-O.

Gao, B.-C., M. Montes, C. Davis, and A. Goetz (2009). Atmospheric correction algorithms for hyperspectral remote sensing data of land and ocean, Remote Sens. of Environ., 113, 17-24. doi:10.1016/j.rse.2007.12.015.

Green, R. O., et al. "The Moon Mineralogy Mapper (M3) imaging spectrometer for lunar science: Instrument description, calibration, on-orbit measurements, science data calibration and on-orbit validation." Journal of Geophysical Research: Planets 116.E10 (2011).

Green, R.O., Eastwood, M.L., Sarture, C.M., Chrien, T.G., Aronsson, M., Chippendale, B.J., Faust, J.A., Pavri, B.E., Chovit, C.J., Solis, M.S., et al. (1998). Imaging spectroscopy and the Airborne Visible Infrared Imaging Spectrometer (AVIRIS). *Remote Sensing of Environment, 65*, 227-248.

Hamlin, L., Green, R.O., Mouroulis, P., Eastwood, M., Wilson, D., Dudik, M., & Paine, C. (2011). Imaging spectrometer science measurements for Terrestrial Ecology: AVIRIS and new developments. In, *Aerospace Conference, 2011 IEEE* (pp. 1 - 7).

Hampton, D.L., Baer, J.W., Huisjen, M.A, Varner, C.C., Delamere, A., Wellnitz. D.D., A'Hearn, M.F., Klaasen, K.P. (2005). An Overview of the Instrument Suite for the Deep Impact Mission, Space Science Reviews, Volume 117, Issue 1, pp 43-93.

Keymeulen, D., N. Aranki, A. Bakhshi, H. Luong, C. Sarture, D. Dolman (2014). Airborne Demonstration of FPGA implementation of Fast Lossless Hyperspectral Data Compression System, Adap. Hard. Sys. Conf., 278-284. doi:10.1109/AHS.2014.6880188.

Kirschke, S., P. Bousquet, et al. (2013). "Three decades of global methane sources and sinks." Nature Geoscience 6(10): 813-823.

Klimesh, M. (2006). Low-Complexity Adaptive Lossless Compression of Hyperspectral Imagery, Proc. SPIE Optics & Photonics Conference, 6300, 9. doi:10.1117/12.682624.

Kort , E., (2014), C. Frankenberg, K.R. Costigan, R. Lindenmaier, M. K. Dubey, D. Wunch, "Four Corners: the largest US methane anomaly viewed from space", GRL. doi: 10.1002/2014GL061503

,

Krings, T., Gerilowski, K., Buchwitz, M., Hartmann, J., Sachs, T., Erzinger, J., Burrows, J. P., and Bovensmann, H.: Quantification of methane emission rates from coal mine ventilation shafts using airborne remote sensing data, Atmos. Meas. Tech., 6, 151–166.

Lee, Christine M., et al. "An introduction to the NASA Hyperspectral InfraRed Imager (HyspIRI) mission and preparatory activities." Remote Sensing of Environment 167 (2015): 6-19.

Lyon, D.R., Zavala-Araiza, D., Alvarez, R.A., Harriss, R., Palacios, V., Lan, X., Talbot, R., Lavoie, T., Shepson, P., Yacovitch, T.I., Herndon, S.C., Marchese, A.J., Zimmerle, D., Robinson, A.L., and Hamburg, S.P. (2015). Constructing a Spatially Resolved Methane Emission Inventory for the Barnett Shale Region. Environmental Science & Technology 2015 49 (13), 8147-8157.

Middleton EM, Ungar SG, Mandl DJ, Ong L, Frye SW, Campbell PE, Landis DR, Young JP, Pollack NH. The earth observing one (EO-1) satellite mission: Over a decade in space. Selected Topics in Applied Earth Observations and Remote Sensing, IEEE Journal of. 2013 Apr;6(2):243-56.

Mouroulis, P., R. O. Green, B. Van Gorp, L. B. Moore, D. W. Wilson, H. Bender (2016): "Landsat swath imaging spectrometer design", Optical Engineering 55(1) 015104 doi:10.1117/1.OE.55.1.015104.

Murchie, S., et al. "Compact reconnaissance imaging spectrometer for Mars (CRISM) on Mars reconnaissance orbiter (MRO)." Journal of Geophysical Research: Planets 112.E5 (2007).

NRC. 2013. Landsat and Beyond: Sustaining and Enhancing the Nation's Land Imaging Program, Washington, D.C.

NRC. 2007. Earth Science and Applications from Space: National Imperatives for the Next Decade and Beyond. Vol. 8. Washington, D.C.

Roberts, D.A., Bradley, E.S., Cheung, R., Leifer, I., Dennison, P.E., & Margolis, J.S. (2010). Mapping methane emissions from a marine geological seep source using imaging spectrometry. *Remote Sensing of Environment, 114*, 592-606.

Schaefer, H., S. E. M. Fletcher, et al. (2016). "A 21st-century shift from fossil-fuel to biogenic methane emissions indicated by (CH4)-C-13." Science 352(6281): 80-84.

Schimel, D., Sellers, P., Moore, B., Carbon., N., et al. (2015). Carbon and Climate:A response to the Request for Information from the Carbon and Climate workshop, Norman,Oklahoma (RFI#1).

Schneising, O., J. P. Burrows, R. R. Dickerson, M. Buchwitz, M. Reuter, H. Bovensmann, Remote sensing of fugitive methane emissions from oil and gas production in North American tight geologic formations, Earth's Future, 2, DOI: 10.1002/2014EF000265, pp. 11, 2014.

Spinetti, C., Carrere, V., Buongiorno, M.F., Sutton, A.J., & Elias, T. (2008). Carbon dioxide of Pu'u'O'o volcanic plume at Kilauea retrieved by AVIRIS hyperspectral data. *Remote Sensing of Environment, 112*, 3192-3199.

Thompson, D.R. et al. (2016). Space-based remote imaging spectroscopy of the Aliso Canyon CH_4 super-emitter. Manuscript under review.

Thompson, D.R., Leifer, I., Bovensmann, H., Eastwood, M., Fladeland, M., Frankenberg, C., Gerilowski, K., Green, R.O., Kratwurst, S., Krings, T., et al. (2015). Real-time remote detection and measurement for airborne imaging spectroscopy: a case study with methane. *Atmos. Meas. Tech., 8*, 4383-4397.

Thompson, David R., et al. "Atmospheric correction for global mapping spectroscopy: ATREM advances for the HyspIRI preparatory campaign." Remote Sensing of Environment 167 (2015): 64-77.

Thorpe, A. K., Frankenberg, C., Green, R. O., Thompson, D. R., Aubrey, A. D.,Mouroulis, P., Matheou, G. (2016). The Airborne Methane Plume Spectrometer (AMPS): Quantitative imaging of methane plumes in real time. Aerospace Conference, 2016 IEEE.

Thorpe, A. K., Frankenberg, C., Aubrey, A. D., Roberts, D. A., Nottrott, A. A., Rahn, T. A., Sauer, J. A., Dubey, M. K., Costigan, K. R., Arata, C., Steffke, A. M., Hills, S., Haselwimmer, C., Charlesworth, D., Funk, C. C., Green, R. O., Lundeen, S. R., Boardman, J. W., Eastwood, M. L., Sarture, C. M., Nolte, S. H., Mccubbin, I. B., Thompson, D. R., McFadden, J. P. (2016). Mapping methane concentrations from a controlled release experiment using the next generation Airborne Visible/Infrared Imaging Spectrometer (AVIRIS-NG). *Remote Sensing of Environment, 179*, 104-115.

Thorpe, A.K., Frankenberg, C., Aubrey, A.D., Roberts, D.A., Roberts, D.A., Nottrott, A.A., Rahn, T.A., Sauer, J.A., Dubey, M.K., Costigan, K.R., et al. (2015). Mapping methane concentrations from a controlled release experiment using the next generation Airborne Visible/Infrared Imaging Spectrometer (AVIRIS-NG) *Remote Sensing of Environment.*

Thorpe, A.K., Frankenberg, C., & Roberts, D.A. (2014). Retrieval techniques for airborne imaging of methane concentrations using high spatial and moderate spectral resolution: Application to AVIRIS. *Atmospheric Measurement Techniques, 7*, 491-506.

Turner, A. J., Jacob, D. J., Wecht, K. J., Maasakkers, J. D., Lundgren, E., Andrews, A. E., Biraud, S. C., Boesch, H., Bowman, K. W., Deutscher, N. M., Dubey, M. K., Griffith, D. W. T., Hase, F., Kuze, A., Notholt, J., Ohyama, H., Parker, R., Payne, V. H., Sussmann, R., Sweeney, C., Velazco, V. A., Warneke, T., Wennberg, P. O., and Wunch, D. (2015): Estimating global and North American methane emissions with high spatial resolution using GOSAT satellite data, Atmos. Chem. Phys., 15, 7049-7069.

Ungar, Stephen G., et al. "Overview of the earth observing one (EO-1) mission." Geoscience and Remote Sensing, IEEE Transactions on 41.6 (2003): 1149-1159.

Ummel, K. 2012. CARMA revisited: an updated database of carbon dioxide emissions from power plants worldwide. Center for Global Development, Working Paper 304.

Vane, Gregg, Alexander FH Goetz, and John B. Wellman. "Airborne imaging spectrometer: A new tool for remote sensing." Geoscience and Remote Sensing, IEEE Transactions on 6 (1984): 546-549.

Veefkind, J. P., Aben, I., McMullan, K., Förster, H., De Vries, J., Otter, G., ... & Van Weele, M. (2012). TROPOMI on the ESA Sentinel-5 Precursor: A GMES mission for global observations of the atmospheric composition for climate, air quality and ozone layer applications. Remote Sensing of Environment, 120, 70-83.

Van Gorp, B., P. Mouroulis, D. W. Wilson, R. O. Green, (2014): “Design of the Compact Wide Swath Imaging Spectrometer (CWIS)”, Proc. SPIE 9222, 92220C, doi:10.1117/12.2062886.Wheeler, D. and Ummel, K. 2008. Calculating CARMA: global estimation of CO2 emissions from the power sector. Center for Global Development, Working Paper 145.

Wheeler, D. and Ummel, K. 2008. Calculating CARMA: global estimation of CO2 emissions from the power sector. Center for Global Development, Working Paper 145.

Zavala-Araiza, D., Lyons, D., Alvarez, R.A., Palacios, V., Harriss, R., Lan, X, Talbot, R., Hamburg, S.P. (2015). "Toward a Functional Definition of Methane Super-Emitters: Application to Natural Gas Production Sites." Environmental Science & Technology, 49, 8167–8174.